

Figures and Preliminary Results

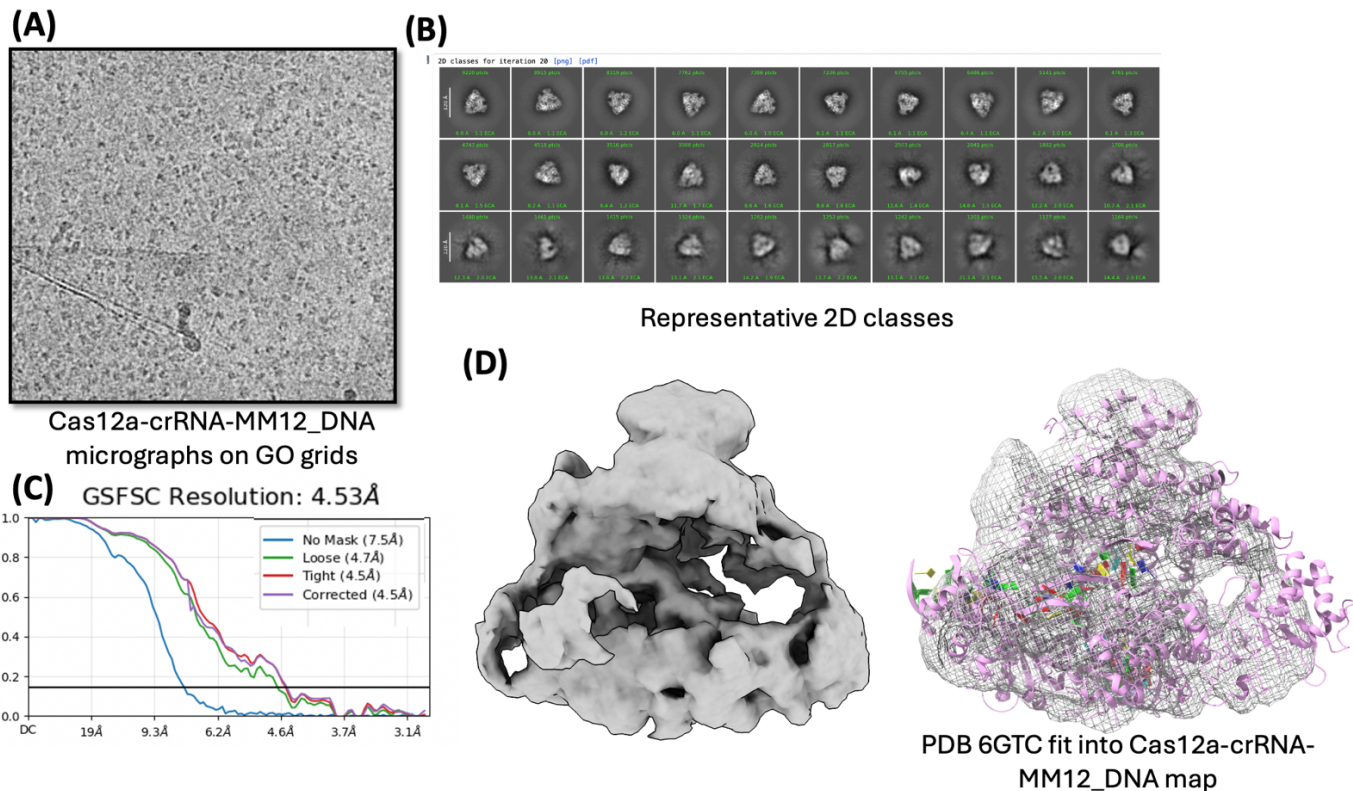


Figure 1. Cryo-EM structure determination of FnoCas12a-BH variant bound to crRNA and a DNA with a mismatch between the crRNA and the DNA. (A) Particle distribution on a grid. (B) 2D class averages of FnoCas12a-KD2P-RNA-DNA complex. (C) Graph showing the gold-standard Fourier shell correlation curves for the dataset. The corrected map is at 4.5Å resolution. (D) An *ab-initio* map and the map with a model derived from PDB ID 6GTG¹ fit into the map. The map shows the general features of the crab-claw shaped FnoCas12a-gRNA-DNA ternary complex. Current work is to collect data with DNA containing different mismatches to delineate the mechanism by which bridge helix contributes to DNA mismatch sensitivity.

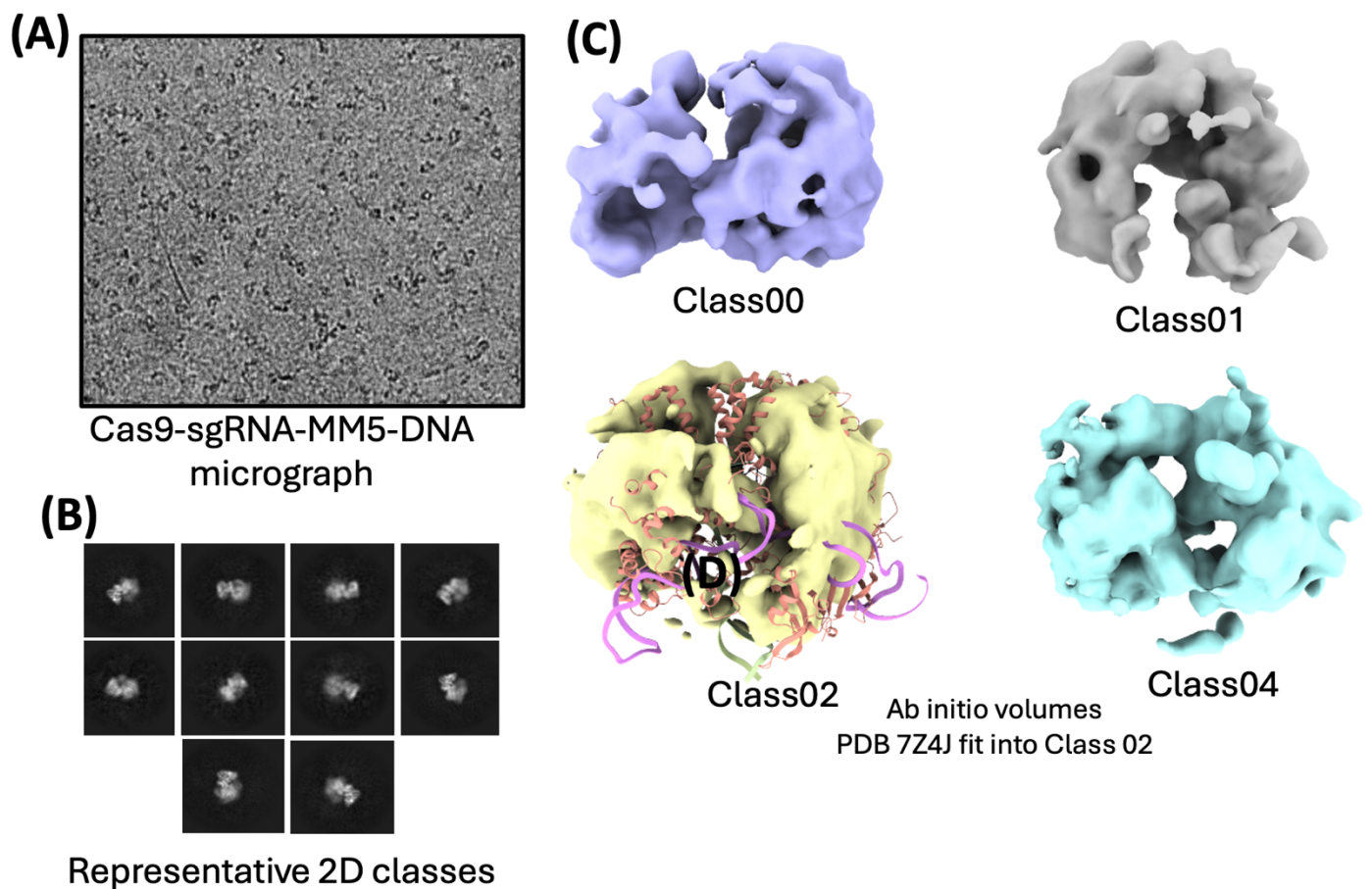


Figure 2. Cryo-EM structure determination of Cas9 variant bound to crRNA and a DNA with a mismatch between the crRNA and the DNA. (A) Particle distribution on a grid. (B) Representative 2D classes for the SpyCas9-2Pro^{2,3}-gRNA-23-mer DNA with a mismatch. (C) Different classes obtained during *ab initio* reconstruction. A model of Cas9-gRNA-DNA (PDB ID: 7Z4J)⁴ is fit into one class. The volumes appear smaller than the model and the 2D classes show limited distribution. We suspect orientation bias and lower stability of the ternary complex that will be addressed through sample and grid preparation and through tilted data collection.

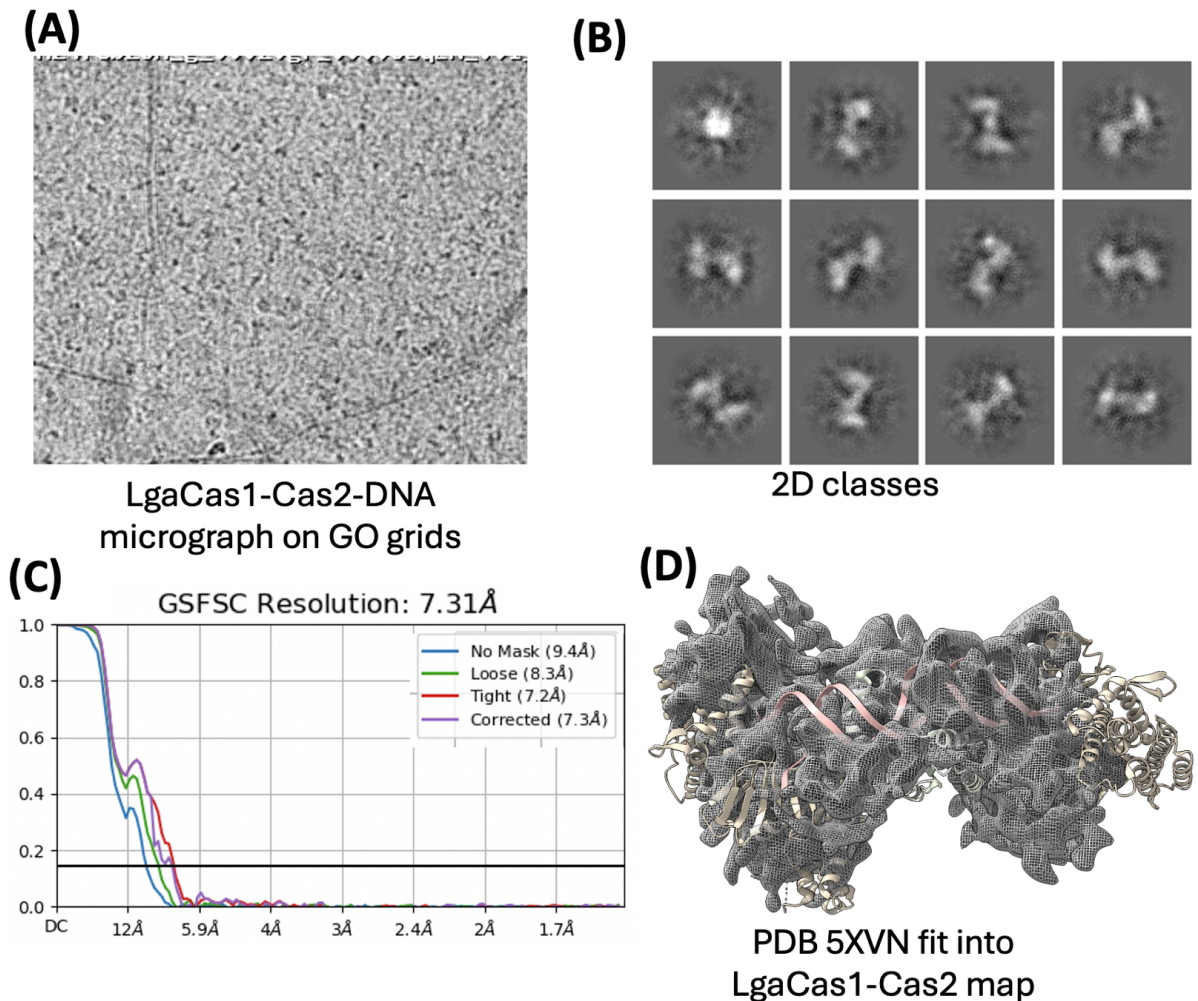


Figure 3. Cryo-EM structure determination of *Lactobacillus gasseri* (Lga) Cas1-Cas2 complex. (A) Particle distribution on a grid. (B) Representative 2D classes. (C) Graph showing the gold-standard Fourier shell correlation curves for the dataset. The corrected map is at 7.3Å resolution. (D) An *ab-initio* map with a model from another ortholog (PDB ID 5XVN)⁵ fit into the map. The map possesses a dumbbell shaped morphology similar to that of the ortholog. Current work is to stabilize the complex and collect more data to increase the resolution of the map.

References Cited:

1. Stella, S., Mesa, P., Thomsen, J., Paul, B., Alcon, P., Jensen, S.B., Saligram, B., Moses, M.E., Hatzakis, N.S. & Montoya, G. Conformational Activation Promotes CRISPR-Cas12a Catalysis and Resetting of the Endonuclease Activity. *Cell* **175**, 1856-1871 e21 (2018).
2. Babu, K., Amrani, N., Jiang, W., Yogesha, S.D., Nguyen, R., Qin, P.Z. & Rajan, R. Bridge helix of Cas9 modulates target DNA cleavage and mismatch tolerance. *Biochemistry* **58**, 1905-1917 (2019).
3. Babu, K., Kathiresan, V., Kumari, P., Newsom, S., Parameshwaran, H.P., Chen, X., Liu, J., Qin, P.Z. & Rajan, R. Coordinated actions of Cas9 HNH and RuvC nuclease domains are regulated by the bridge helix and the target DNA sequence. *Biochemistry* **60**, 3783-3800 (2021).
4. Pacesa, M., Loeff, L., Querques, I., Muckenfuss, L.M., Sawicka, M., Jinek, M. R-loop formation and conformational activation mechanisms of Cas9. *Nature* **609**: 191-196 (2022)
5. Xiao, Y., Ng, S., Nam, K.H. & Ke, A. How type II CRISPR-Cas establish immunity through Cas1-Cas2-mediated spacer integration. *Nature* **550**, 137-141 (2017).